Calculation of Optimal Luminaires for Architectural Design

Rodrigo Leira[1], Eduardo Fernández[1] and Gonzalo Besuievsky[2]
[1]*Centro de Cálculo, Universidad de la República, Montevideo, Uruguay*
[2]*Geometry and Graphics Group, Universitat de Girona, Girona, Spain*

Keywords: Inverse Lighting, Radiosity, Photometric Data, Luminaires.

Abstract: The selection and location of optimal luminaries is a central aspect of architectural design. Its complexity arises due to the diversity of existing luminaires, and the problems related to the need of achieving a set of lighting goals and constraints. The use of computer simulation software can bring an improved support in decision making at design time. CAD applications for illumination assessment are generally based on a working forward strategy, where the designer selects all the design elements, in order to calculate the resulting illumination. In this paper we present an inverse approach for the selection of luminaires, where the designer defines a set of lighting intentions to satisfy, and then an optimization algorithm iterates, converging to a feasible and optimal solution. The method allows to use a database consisting of hundreds of luminaires and a set of possible locations. In each iteration, after the first reflection of a potential configuration is calculated, the radiosity method is used to compute the final illumination of the scene.

1 INTRODUCTION

The selection and the location of luminaires are important steps in the process of architectural design. Its complexity arises from the need of satisfying a set of goals and constraints to ensure the efficiency, appeal, and functionality aspects of the resulting environment. These set of constraints and goals are defined as Lighting Intentions (LIs) (Russell, 2012). The problem of finding the illumination settings from LIs is known as inverse lighting problem (ILP) (Marschner, 1998). Given its multiple factors, the designer must adjust each of the variables involved with the aim of satisfying the LIs. This is not a new dilemma and existing professional illumination CAD tools, as for example Dialux (DIALux, 2016), provide tools that can serve this meaning. The main deficiency of these is that they are based on a forward strategy that it is not appropriate for optimization. Because of this, a computer simulation module that is able to compute optimal solutions, can provide great support.

We present a novel optimization method for ILP that considers the position and main luminaire characteristics (spatial and power distribution), to find the optima for a given set of LIs. The method is based on a low-rank approximation of the radiosity matrix (Fernández, 2009) and the search of the optima by means of the VNS (Variable Neighborhood Search) meta-heuristic (Mladenović and Hansen, 1997).

This paper proposes a technique that allows considering the way different types of luminaires emit light, in the optimization process. The data of luminaires is taken from databases provided by manufacturers and is used to produce the first light reflection on the scene. Then, the low-rank radiosity (LRR) method is used as an efficient engine to calculate the final radiosity.

2 RELATED WORK

The technique presented deals with an inverse lighting problem that infers the properties of a physical system from desired data. Inverse problems are ill-posed and of interest in a wide range of fields in lighting engineering and lighting design. We use the radiosity computation with the goal of solving such inverse problems looking for a global illumination solution. This is partially based on the work done in (Fernández and Besuievsky, 2012), where the LRR method is used to solve the inverse lighting problem.

In the context of luminaire optimizations, many methods have been developed to optimize the position of a set of luminaires in a scene in order to produce an approximation to the optimal lighting design. In (Shikder et al., 2010) a method is formulated for placing two fixed luminaires into two separated sets of positions. They consider the photometric values of the

Leira R., FernÃąndez E. and Besuievsky G.
Calculation of Optimal Luminaires for Architectural Design.
DOI: 10.5220/0006102702030211
In *Proceedings of the 12th International Joint Conference on Computer Vision, Imaging and Computer Graphics Theory and Applications (VISIGRAPP 2017)*, pages 203-211
ISBN: 978-989-758-224-0

luminaire but use two fixed luminaires that can be positioned on two disjoint set of points and optimize its positioning. Other approach, similar to the previous method, is introduced in (Uygun et al., 2015) for optimizing a set of luminaire positions. They also consider the luminaire photometric data but without any optimization performance. An interesting method is presented for designing exterior lighting for building in (Schwarz and Wonka, 2014) where they optimize position, rotation and luminaire distribution but only consider direct illumination and a reduced database of luminaires.

2.1 Photometric Files and Polar Curves of Luminaires

The presented approach focuses on calculating a first reflection of the light emmited by the luminaire into the geometry of the scene. That first reflection is then used as the emission on the radiosity method. In order to map the first reflection into the scene the polar curve is used. The polar curves are taken from photometric files, which are defined with the LM-63-02 IESNA standard (IESNA-Computer-Committee, 1995) or its equivalent EULUMDAT format. Data from these files have to be transformed to represent the incident luminous flux (measured in lumens) recieved by a given patch in the scene. In this report we use a database composed of 1516 luminaires extracted from (Philips, 2016) and (Cree, 2016).

2.2 LRR

The method presented assumes that all surfaces in the scenes are Lambertian reflectors. This assumption allows to speed up the calculations, evaluating thousands of luminaires configurations in a short time. Our solver is based on the radiosity problem, taking as emission the first reflection calculated using the polar curves.

The discrete radiosity equation is formulated as:

$$(\mathbf{I}-\mathbf{RF})B = E \tag{1}$$

where E is a vector containing the light emissions for each patch in the scene, $\mathbf{I}$ is the identity matrix, $\mathbf{R}$ is a diagonal matrix containing the diffuse reflectivity for each patch. $\mathbf{F}$ is a matrix containing the form factors, where $\mathbf{F}(i,j)$ is a value between 0 and 1 indicating the proportion of the total light radiated by the patch i going to patch j. B is a vector containing the radiosity values to be found (Cohen et al., 1993). LRR takes into consideration the low-rank properties of the **RF** matrices (Fernández, 2009). **RF** size is $O(n^2)$ but due to the spatial coherence of the radiosity values, i.e. close patches typically have similar radiosity values, **RF** can be approximated by the product $\mathbf{UV}^T$ where $\mathbf{U}$ and $\mathbf{V}$ are $n \times k$ matrices that can be computed applying $O(n^2)$ operations, where $n \gg k$. Further, $\mathbf{U}$ is a dense matrix and $\mathbf{V}$ is a sparse matrix. In addition to the previous approximation, the Sherman-Morrison-Woodbury (Golub and Van Loan, 2013) formula is used to calculate an approximation of the inverse of the radiosity matrix $\mathbf{M}$:

$$\mathbf{M} = (\mathbf{I}-\mathbf{RF})^{-1} \approx (\mathbf{I}+\mathbf{YV}^T) = \tilde{\mathbf{M}} \tag{2}$$
$$\text{where} \quad \mathbf{Y} = \mathbf{U}(\mathbf{I}-\mathbf{V}^T\mathbf{U})^{-1}$$

Then we can reduce Eq. (1) to the following matrix-vector product: $\tilde{B} = \tilde{\mathbf{M}}E$, which can be also formulated as:

$$\tilde{B} = E + \mathbf{Y}(\mathbf{V}^T E) \tag{3}$$

In this equation, $\tilde{B}$ is an approximation of B. This final reduction grants the ability of calculating $\tilde{B}$ in $O(nk)$ operations and consuming $O(nk)$ memory. The benefits of this are straightforward, on the condition that the scene geometry does not change. This method can be used to solve inverse lighting problems, gaining a speed up over traditional radiosity methods, allowing us to calculate the radiosity of static scenes containing thousands of elements, and allowing the changing of the emitters. Like this, other methods have been proposed to speed up the calculations of $\mathbf{Y}$ and $\mathbf{V}$ (Aguerre and Fernández, 2016).

2.3 Optimization Problem

The ILP is determined as the process of placing the emitters in order to achieve a set of Lighting Intensions. This process was proposed as an alternative to solving Eq. (1), which results in an ill-posed linear system because of the low-rank properties of the **RF** matrix (Fernández and Besuievsky, 2015).

VNS is the method used for seeking for optimal configurations. The main idea of VNS is the successive exploration of neighborhoods (usually nested), where a finite and random set of representatives is selected with the intention of finding a solution that is better than the best found on previous iterations. What is interesting about this method is that it walks from neighborhood to neighborhood in a systematic fashion in order to escape from local optima, and therefore improving odds of finding the global optima (Talbi, 2009).

2.4 Hemi-cube

The presented approach uses a hemi-cube to calculate the emission from a luminaire into the scene. The

hemi-cube method used is based on the concept first introduced by (Cohen and Greenberg, 1985). On Cohen proposal the hemi-cube consists of 5 projections, or faces, divided into many pixels where the patches of the scene are projected. For each pixel the $\Delta\mathbf{F}$ is calculated as viewed from the center of the patch where the hemi-cube is positioned. Given the hemi-cube centered on the barycenter of patch i, onto which a patch j is projected, the sum of the $\Delta\mathbf{F}$ (form factors) associated to patch j is $\mathbf{F}(i, j)$. This summation is performed for each patch obtaining a vector with all form-factors for the scene for the hemi-cube positioned at patch i. When many patches of the scene are projected onto the same pixel of the hemi-cube, the patch seen in that pixel is determined by calculating the distance to patch i and selecting the nearest. We use a variation of the form factors where each pixel is associated to its delta solid angle ($\Delta\Omega$), see Section 3.3. This information can be used altogether with the information taken from photometric files to build the first reflection of the light in the scene.

3 METHOD OVERVIEW

The pipeline design of the proposed approach is described in Fig. 1. It starts from a given architectural interior model for lighting design with reflectance surfaces already defined. Then the user configures the parameters to specify the zones where the light sources can be placed as well as the variables to optimize. This includes the geometric restrictions and other lighting intentions to achieve, as for instance, the goals and constraints related to energy consumption, with the aim of finding the optimal solution. Also the database containing the desired set of luminaries is provided. Then the precomputation process provides the hemi-cubes needed for the optimization as well as the matrices obtained from the LRR method. Next, the optimization process is executed to find a candidate configuration, which is evaluated by the designer. Regarding the resulting values, the designer can modify the setting parameters in order to search for a new solution.

3.1 Precomputation

Before the optimization process begins, a precomputation process is executed (see Fig. 2). A compact representation of the scene information is obtained by means of the LRR method. Also, the database with the photometric files is preprocessed in order to create the hemi-cube **L** associated to each polar curve. Next, the process of creating each hemi-cube view **H**

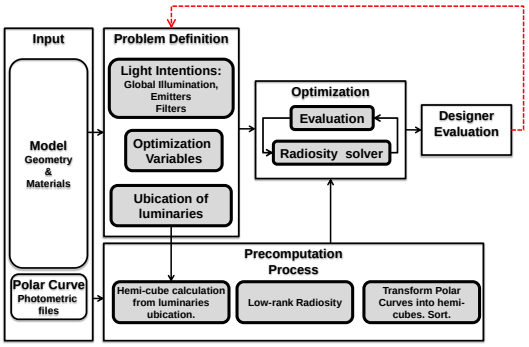

Figure 1: Pipeline system.

for the scene from each possible luminaire location is performed. These hemi-cubes are calculated using the z-buffer technique and a color based encoding for the patch indexes (see Fig. 3). Both **L** and **H** are represented as matrices.

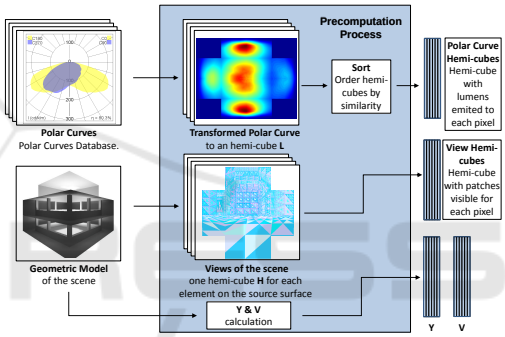

Figure 2: Precomputation process. Hemi-cubes **L**'s and **H**'s are generated, as well as **Y** and **V** matrices. **L**'s are sorted (Algorithm 1).

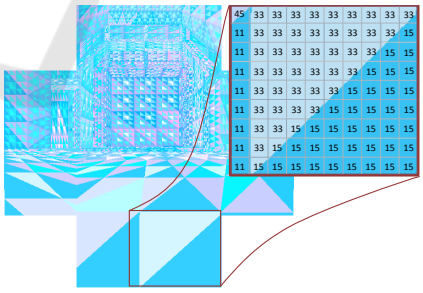

Figure 3: Hemi-cube view of the scene **H**. The colors encode the index for each patch. In the top-right, the index associated to each pixel is displayed.

The proposed method uses the VNS metaheuristic, therefore, we need to sort the **L**'s and **H**'s hemi-cubes in a way that allows to build the neighborhoods. For the **H**'s views, the neighborhoods are built using their positions. The neighbors of an location are those positions that are close in space. On the other hand, to calculate the neighborhoods for the hemi-cubes based on polar curves, we use the Euclidean

distance (Frobenius norm) to sort them by means of Algorithm 1.

Algorithm 1: Sort luminaires hemi-cubes.

Require: **D** # **D** is a n×n distance matrix
1: $I \leftarrow [1{:}n]$
2: **for** k=1:n-1 **do**
3: $\mathbf{subD}_k \leftarrow \mathbf{D}(1{:}k, k{+}1{:}n)$
4: $(min, i, j) \leftarrow minimum(\mathbf{subD})$
5: **if** $min < \delta$ **then**
6: $\mathbf{D} \leftarrow moveCol(\mathbf{D}, j, i)$
7: $\mathbf{D} \leftarrow moveRow(\mathbf{D}, j, i)$
8: $I \leftarrow move(I, j, i)$
9: **else**
10: $\mathbf{D} \leftarrow moveCol(\mathbf{D}, j, k)$
11: $\mathbf{D} \leftarrow moveRow(\mathbf{D}, j, k)$
12: $I \leftarrow move(I, j, k)$
13: **end if**
14: **end for**
15: **return** I

The sorting algorithm receives a matrix **D** as input, where $\mathbf{D}(i,j)=||\mathbf{L}_i-\mathbf{L}_j||_{Fr}$, is the Euclidean distance between the hemi-cubes of luminaires i and j. In the k^{th} step, $I(1{:}k)$ is a list of sorted luminaires, and $I(k{+}1{:}n)$ is the remaining set of unsorted luminaires. When adding a new luminaire to the sorted list, an unsorted luminaire j is chosen such that it minimizes the distance to any luminaire in the sorted list. To do so, the first step (line 3) takes the matrix $\mathbf{subD}_k$ that contains all the distances between both sets. Then the luminaires i and j are selected such that i belongs to the sorted list and j to the unsorted set, and its Euclidean distance is minimal (line 4 and Fig. 4). If that distance is less than a predefined threshold δ, then luminaire j is placed in the sorted list between the luminaires i and $i{+}1$ (lines 6 to 8 and Fig. 5 (a)), otherwise it is located at the end of the sorted list (lines 10 to 12 and Fig. 5 (b)). The algorithm starts including one luminaire in the sorted list, and at each step a new element is added to it. For the unsorted set the opposite happens. It starts with all the luminaires but the one selected, and at each step one element is extracted. At the end, all the luminaires belong to the sorted list. Finally the algorithm returns a vector with the sorted indexes (line 15). In this vector, the position i contains the index of the i^{th} luminaire in the sorted list.

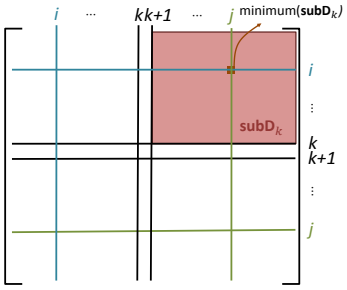

Figure 4: $\mathbf{subD}_k$ contains the distances between the sorted and unordered luminaires. $\mathbf{subD}_k(i,j)$ contains the minimum distance between them. The minimum value on the sub-matrix is selected.

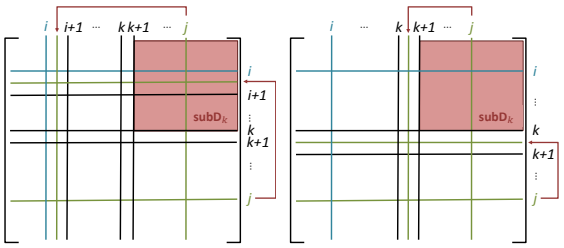

(a) $min < \delta$ (b) $min \geq \delta$

Figure 5: Sorting steps. Relocation of i row and j column.

An example with the result of sorting the selected luminaires (Sec. 2.1) can be seen in Fig. 6. It can be observed that a greater similarity exists between consecutive columns on the sorted list.

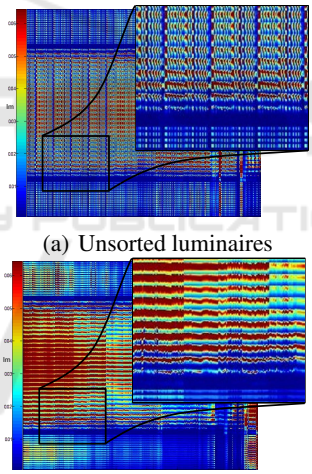

(a) Unsorted luminaires

(b) Sorted luminaires

Figure 6: Plot of the database containing the luminaire hemi-cubes. In the image, each column represents a hemi-cube (reshaped as a vector).

3.2 Optimization

The optimization process (see Fig. 1) initializes the set of variables using a random seed. Using VNS we search for variables in the same neighborhood to the ones selected, using the positions and the list of sorted luminaires calculated on the precomputation process. In each step, the hemi-cubes $\mathbf{H}_i$ and $\mathbf{L}_l$ of a selected view i and a luminaire l are combined to calculate the lumens received for each patch as the

first reflection. The luminous emittance is then calculated, using the direct luminous emittance (first reflection) as the emission on the radiosity equation (see Eqs. (1) and (3)). After that, the illumination is compared to the best solution found, following the VNS meta-heuristic.

3.3 Direct Luminous Emittance Calculation

In this section we focus on achieving a first reflection that is used as emission in the radiosity equation. In order to construct it, we use the hemi-cube technique in conjunction with the information contained in the photometric files.

Eq. (4) shows how to obtain the direct luminous emittance $E_{i,l}(p)$ of each patch p on the scene, given a luminaire l positioned at patch i:

$$E_{i,l}(p) = \frac{R(p)}{A(p)} \sum_{\substack{\{(u,v):\\ \mathbf{H}_i(u,v)=p\}}} \mathbf{\Delta\Omega}(u,v)\mathbf{L}_l(u,v) \quad (4)$$

where p is a patch on the scene, $R(p)$ is its diffuse reflectivity, $A(p)$ is its area, $\mathbf{H}_i$ is the hemi-cube view of the scene (Fig. 3), in the matrix $\mathbf{\Delta\Omega}$ each of its elements (u,v) contains the solid angle, measured in sr, of pixel (u,v) (Fig. 7). $\mathbf{L}_l(u,v)$ contains the number of candelas transmitted through pixel (u,v) by the luminaire l. $\mathbf{L}_l(u,v)$ is built using the information provided in polar curves, assigning the value corresponding to the emission in candelas (lm/sr) of the luminaire to each pixel. The patch seen through each pixel on hemi-cube $\mathbf{H}_i$ is determined using the z-buffer algorithm.

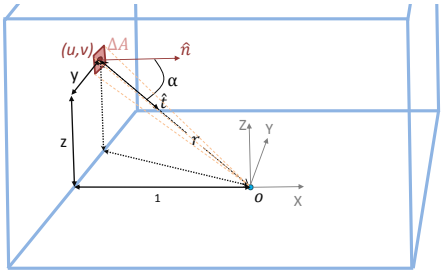

Figure 7: ΔΩ calculation of pixel (u,v).

Each addend $\mathbf{\Delta\Omega}(u,v)\mathbf{L}_l(u,v)$ of Eq. (4) determines the luminous flux (i.e. the number of lumens) that are transmitted through pixel (u,v) and the whole sum is the incident luminous flux (lm) on patch p.

Each $\mathbf{\Delta\Omega}(u,v)$ is determined by Eq. (5):

$$\mathbf{\Delta\Omega}(u,v) = \frac{4\pi\Delta A}{A_s}\,\hat{t}\cdot\hat{n} \quad (5)$$

where ΔA is the area of pixel (u,v), A_s is the area of the sphere of radius r centered on point o ($4\pi r^2$), $\hat{n}$ is a unit vector normal to the pixel, and $\hat{t}$ is a unit vector centered on the pixel with a radial direction. The scalar product $\hat{t}\cdot\hat{n}$ determines the cosine of α. Therefore Eq. (5) can be expressed as follows:

$$\mathbf{\Delta\Omega}(u,v) = \frac{4\pi\Delta A}{4\pi(x^2+y^2+z^2)}\,\frac{1}{\sqrt{x^2+y^2+z^2}} \quad (6)$$

because $r^2 = x^2+y^2+z^2$, and $\hat{t}\cdot\hat{n} = \dfrac{1}{\sqrt{x^2+y^2+z^2}}$

resulting in Eq. (7):

$$\mathbf{\Delta\Omega}(u,v) = \frac{\Delta A}{(x^2+y^2+z^2)^{\frac{3}{2}}} \quad (7)$$

The sum of all $\mathbf{\Delta\Omega}(u,v)$ equals 2π. Finally, since $E_{i,l}$ is the direct luminous emittance (lx), then the incident luminous flux on patch p is divided by $A(p)$ (which determines the direct illuminance) and multiplied by reflectivity $R(p)$.

4 IMPLEMENTATION

In order to reduce the resources needed for our method, or to achieve better results in some cases, we use the following implementation strategies:

Tabu Search: We use the Tabu Search method to discourage the coming back to previously-visited solutions (Glover and Laguna, 1997).

Empty Luminaire: Since we are optimizing the configuration of luminaires it seems to be a good idea to introduce the concept of an empty luminaire. This luminaire emits no light and is used to relax the number of luminaires marked by the designer. In this way the optimization process is allowed to use empty luminaires that consumes 0 watts, so that it is possible to achieve configurations with less luminaires. This is performed by adding a hemi-cube L_0 filled with zeros (no emission).

Probability of Change for Variables: We use three variables to configure a luminaire, one for the luminaire index and two for its location. When searching for a candidate within the current VNS neighborhood, the neighborhood establishes the number of variables that can be changed at the same time. Since the cardinality for the domain of each of these variables is different, a higher chance of change is given to the variable of larger cardinality.

Polar Curve Hemi-cube: We focus on calculating the emission for the lower half space only. This is implemented with the hemi-cube $\mathbf{L}$.

5 EXPERIMENTS AND RESULTS

Different experiments are performed in the literature (Shikder et al., 2010; Uygun et al., 2015; Fernández and Besuievsky, 2014) to validate their particular results. The experiments chosen are used to satisfy some useful lighting standards, as well as to consider realistic objectives and constraints for design. In all experiments performed in this section, the luminaires are placed on the roof of a patio scene (see Fig. 8) The target surface for measuring light uniformity (for Section 5.2) and power efficiency (for Section 5.3), are the patches that defines the floor of the patio. All experiments use a database consisting of 1517 hemi-cubes $\mathbf{L}$ (1516 generated from the photometric files and the hemi-cube related to the empty luminaire L_0) is used along with a scene consisting of 21824 triangles. All instances were executed 30 times (independent runs) and all optimizations perform a maximum of 15000 radiosity calculations. The simulations were conducted on a desktop computer, with Intel quad-core i7 processor and 16 Gbytes of RAM. The code was implemented mainly in MATLAB (MATLAB, 2014), also using C++ and OpenGL.

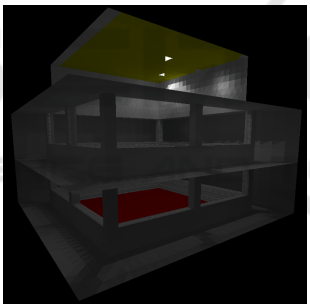

Figure 8: Lighting calculated for the scene. The possible positions of luminaires are colored in yellow and the target surface in red. White patches represent the places where the two luminaires were placed in the rendered configuration.

5.1 Convergence

The first experiment is meant for analyzing the effectiveness of the algorithm. Here we consider as optimization target the radiosity output $\tilde{B}_T$, previously calculated for a given configuration of luminaires and positions. The objective is to minimize the Euclidean distance between the radiosity $\tilde{B}$ of the tested configurations and $\tilde{B}_T$:

$$minimize : \|\tilde{B} - \tilde{B}_T\|_2 \tag{8}$$

The results for this experiment can be seen on Table 1. It shows the number of runs in which the target was found, the mean of the number of radiosity calculations, the mean of the relative error, and the worst relative error found. The algorithm stops when Eq. (8) is 0. For the case of two luminaires, even though the exact solution was found only one time, the mean and worst relative errors show that the solutions are close to the target. The use of three luminaires returned similar results.

Table 1: Optimization results for minimizing the distance to a given lighting.

# lum	# found	$\mu(\#rad)$	$\mu\left(\frac{\|\tilde{B}-\tilde{B}_T\|_2}{\|\tilde{B}_T\|_2}\right)$	$\max\left(\frac{\|\tilde{B}-\tilde{B}_T\|_2}{\|\tilde{B}_T\|_2}\right)$
1	29	5139	3.0×10^{-3}	9.0×10^{-2}
2	1	14876	4.3×10^{-2}	6.0×10^{-2}
3	0	15000	3.1×10^{-2}	5.3×10^{-2}

5.2 Light Uniformity

The achievement of lighting uniformity is an important goal to be considered in the design of lighting systems (Staff et al., 2011). To obtain this goal, the coefficient of variation (σ/μ) is minimized. This coefficient is a normalized measure of dispersion (Canavos, 1984).

$$minimize : \frac{\sigma(\tilde{B})}{\mu(\tilde{B})} \tag{9}$$

This experiment is performed using only one luminaire. The expected result consists in finding a luminaire centered on the roof, with a symmetric polar curve that has greater light intensity on the angles that point to the floor borders. The solutions found can be seen in Fig. 9, where the position found for each solution is centered on the roof (Fig. 9 (a)). The polar curve (Fig. 9 (b)) is symmetric in all planes having greater emission in the angles that are further from the normal (illuminating patches that are more distant). The resulting lighting for the central patch and the luminaire that was selected 29 times from Figs. 9 (a) and (b) respectively, can be seen in Fig. 10.

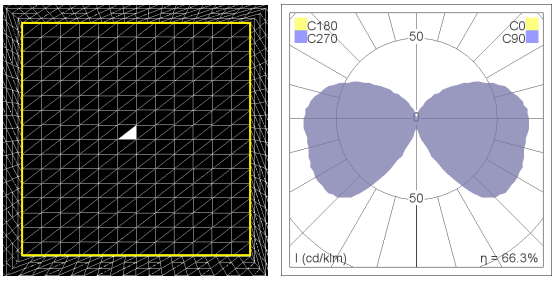

(a) Position selected on the roof, on all runs, marked as a white triangle.

(b) Polar curve found on 29 runs.

Figure 9: Results for optimizing the lighting uniformity.

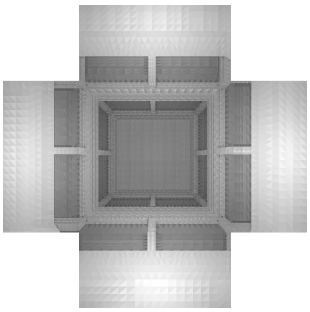

Figure 10: Hemi-cube view of the lighting result when optimizing the uniformity of the floor Section 5.2.

5.3 Power Efficiency

This experiment consists in minimizing the power consumption for luminaires subject to certain illuminance bounds in the target surface:

$$minimize : \sum_{i=1}^{n} P_i \quad , \quad i \in 1..n \tag{10}$$

$$subject\ \ to : \begin{cases} min(I) >= 100\text{lm} \\ max(I) <= 750\text{lm} \end{cases}$$

where n is the number of luminaires placed in the scene, P_i is the power in watts consumed by the i^{th} luminaire and I is a vector containing the illuminance values found in each patch of the target surface. In this test we start from a single luminaire and then we do successive increments by one luminaire. The main idea of this approach is to add new configurations to the space of solutions, leading to better results. The existence of the empty luminaire allows maintaining the solutions of previously explored search spaces to the new space of solutions. Therefore, the addition of luminaires maintains the previous solutions and expands it to include new configurations.

When using a single luminaire, the best solution found consumes 274 W. To validate this solution, we evaluate each adjacent position with all the luminaires of the database. To prove that, the solution found is at least a local optimum. Next, the successive increments in the number of luminaires are executed and improve the solution as expected, see Table 2.

Table 2: Optimization results for different number of luminaires using hemi-cubes of size 512x512. The objective consists in minimizing the power consumption.

# lum	best (W)	worst (W)	$\mu \pm \sigma$ (W)
1 [1]	274	431 [2]	379 ± 75
2	157	174	160 ± 4
3	138	173	154 ± 11
4	125	173	152 ± 10

[1] Not all iterations ended with a valid configuration.
[2] Maximum luminaire power is returned when no valid solution was found.

5.4 Sorting Algorithm

All previous experiments were performed using the sorted **L**'s hemi-cubes, by means of the algorithm introduced in Algorithm 1. Here we perform the experiment for optimizing the power efficiency (Section 5.3) again but without applying the sorting algorithm (using the database as seen in Fig. 5 (b)). Tables 2 and 3 show that the results without applying the sorting algorithm are more power consuming than the ones obtained when using the sorted database.

Table 3: Optimization results for different number of luminaires using hemi-cubes of size 512x512 without sort. The objective consists in minimizing the power consumption.

# lum	best (W)	worst (W)	$\mu \pm \sigma$ (W)
1	431	431	431 ± 0
2	371	442	433 ± 14
3	365	453	417 ± 30
4	365	454	430 ± 23

5.5 Performance

All optimizations performed in this section are based on the same goals and constrains used in the power efficiency experiment (Section 5.3).

Number of Luminaires: The relation between the number of luminaires and the time needed for the optimization process is shown in Table 4, where there is a rough linear relation between them.

Table 4: Optimization results using 512×512 hemi-cubes, after 15000 radiosity calculations each.

# lum	best (s)	worst (s)	$\mu \pm \sigma$ (s)	$\#rad/s$
1	335	398	339 ± 12	44
2	566	717	578 ± 29	26
3	787	827	809 ± 9	19
4	1.0×10^3	1.2×10^3	$1.1 \times 10^3 \pm 12$	14

Hemi-cube Size: Table 5 shows the power of the solutions and timings for different hemi-cube sizes and 4 luminaires. Smaller hemi-cubes results in larger speedups but also in larger errors. This is due to the fact that in general, smaller hemi-cubes contain less accurate information about the scene.

For the precomputation step, an experiment was conducted to measure its execution time for different hemi-cube sizes. In Table 6, the size of the hemi-cube is roughly proportional to the precomputation time.

6 CONCLUSIONS

A new technique is introduced for lighting optimization considering hundreds of luminaires. The

Table 5: Optimization for 4 luminaires and different hemi-cubes.

H	$\mu\pm\sigma$ (W)	$\mu\pm\sigma$ (s)	error	speedup
512×512	152±10	1061±12	-	-
256×256	162±11	408±8	0.068	2.6
128×128	186±13	262±14	0.225	4.1
64×64	260±35	224±13	0.711	4.8

Table 6: Time results for the precomputation process.

H	total time (s)	speedup
512×512	20654	-
256×256	4860	4.3
128×128	1382	14.9
64×64	354	58.3

method is mainly based on the use of the hemi-cube technique, the sorting of luminaires according to their similarity, and the use of an optimization meta-heuristic (VNS). The developed method allows to evaluate thousands of configurations, with a set of more than 1500 luminaires, in few minutes. The convergence of the method was evaluated resulting in a relative error up to 0.043. The relevance of the sorting of luminaires was evaluated and proved to improve the optimization. The technique performed well in tests related to light uniformity and power efficiency. The selection of the hemi-cube size should take into consideration a trade off between the time of the algorithm and the error of the results.

Further steps should include the exploration of other techniques to perform the sorting of the luminaire hemi-cubes, as well as the use of both (upper and lower) hemi-cubes to model luminaire emission. Also it is important to consider the orientation and tilt of the luminaire as optimization variables, since polar curves can be non-symmetrical and so studying further techniques that allow to dynamically rotate the polar curves (maintaining similar performance) is an important step to follow. In order to consider non-Lambertian surfaces it is necessary to explore new rendering techniques that allow to maintain similar performance. Finally, it would be useful to consider the influence of daylighting in the optimization process.

ACKNOWLEDGEMENTS

The work was supported by project FSE_1_2014_1_102344 from Agencia Nacional de Investigación e Innovación (ANII, Uruguay) and project TIN2014-52211-C2-2-R from Ministerio de Economía y Competitividad, Spain.

REFERENCES

Aguerre, J. P. and Fernández, E. (2016). A hierarchical factorization method for efficient radiosity calculations. *Comput Graph*, (to appear).

Canavos, G. (1984). *Applied probability and statistical methods:*. Little, Brown.

Cohen, M. F. and Greenberg, D. P. (1985). The hemi-cube: a radiosity solution for complex environments. In *SIGGRAPH Comput Graph 1985*, pages 31–40.

Cohen, M. F., Wallace, J., and Hanrahan, P. (1993). *Radiosity and Realistic Image Synthesis*. Academic Press Professional, Inc., San Diego, CA, USA.

Cree (2016). Cree europe s.r.l a s.u., http://www.cree-europe.com/en/doc-tecnica-dbf.php.

DIALux (2016). Dial. light building software. www.dial.de.

Fernández, E. (2009). Low-rank radiosity. In *Proc. Iberoamerican Symposium in Computer Graphics (SIACG 2009)*, pages 55–62.

Fernández, E. and Besuievsky, G. (2012). Inverse lighting design for interior buildings integrating natural and artificial sources. *Comput Graph*, 36(8):1096–1108.

Fernández, E. and Besuievsky, G. (2014). Efficient inverse lighting: A statistical approach. *Autom Constr*, 37(Complete):48–57.

Fernández, E. and Besuievsky, G. (2015). Inverse opening design with anisotropic lighting incidence. *Comput Graph*, 47(1):113–122.

Glover, F. and Laguna, M. (1997). *Tabu Search*. Kluwer Academic Publishers, Norwell, MA, USA.

Golub, G. and Van Loan, C. (2013). *Matrix Computations*. Johns Hopkins Studies in the Mathematical Sciences. Johns Hopkins University Press.

IESNA-Computer-Committee (1995). *IESNA standard file format for electronic transfer of photometric data*. IESNA lighting measurements series. IESNA.

Marschner, S. R. (1998). *Inverse Rendering for Computer Graphics*. PhD thesis, Ithaca, NY, USA. AAI9839924.

MATLAB (2014). *version 8.3.0 (R2014a)*. The MathWorks Inc., Natick, Massachusetts.

Mladenović, N. and Hansen, P. (1997). Variable neighborhood search. *Comput. Oper. Res.*, 24(11):1097–1100.

Philips (2016). Philips lighting holding b.v., http://www.lighting.philips.com/main/support/support/dialux-and-other-downloads.html.

Russell, S. (2012). *The Architecture of Light - Architectural Lighting Design Concepts and Techniques*. Conceptnine.

Schwarz, M. and Wonka, P. (2014). Procedural design of exterior lighting for buildings with complex constraints. *ACM Trans. Graph.*, 33(5):166:1–166:16.

Shikder, S. H., Mourshed, M. M., and Price, A. D. F. (2010). Luminaire position optimization using radiance based simulation: a test case of a senior living room. In *Computing in Civil and Building Engineering*.

Staff, B. S. I., Institution, B. S., and for Standardization. CPL/34/10, E. C. (2011). *Light and Lighting -*

Lighting of Work Places: Indoor work places. Part 1. BSI.

Talbi, E.-G. (2009). *Metaheuristics: From Design to Implementation*. Wiley Publishing.

Uygun, I., Kazanasmaz, Z., and Kale, S. (2015). Optimization of energy efficient luminaire layout design in workspaces. In Scartezzini, J.-L., editor, *CISBAT 2015*, pages 301–306, Lausanne. LESO-PB, EPFL.